A Universal 8-Vertex Origami Torus Triangulation

Peter G. Doyle, Fabian Lander,
Richard Evan Schwartz*, Steve Trettel

October 30, 2026

Abstract

An origami torus is a piecewise affine isometric embedding of a flat torus into $\boldsymbol{R}^3$. We prove that every flat torus is realized as an 8-vertex origami torus based on the triangulation with degree sequence $4, 6, 6, 6, 6, 6, 7, 7$. This provides an 8-vertex universal triangulation for origami tori. This initial version of the paper does not explore the beautiful geometry of the objects involved or the theory behind them; it just gets the job done.

1 Introduction

1.1 The Main Result

A *flat torus* is a quotient of the form $T = \boldsymbol{R}^2/\Lambda$, where Λ is a lattice of translations of $\boldsymbol{R}^2$. The lattice Λ is called the *lattice* of T. A *triangulation* τ of a flat torus T is a decomposition of T into finitely many triangles, such that every two triangles are either disjoint, or share one vertex, or share one edge.

Two triangulations τ_1 and τ_2, respectively of flat tori T_1 and T_2, are *combinatorially equivalent* if there is a homeomorphism $h : T_1 \to T_2$ which affinely maps each triangle of τ_1 to a triangle of τ_2. The equivalence class of τ is called its *combinatorial type*. We will sometimes blur the distinction between a triangulation and its combinatorial type. There are 7 different combinatorial types of 8-vertex triangulations of tori. Figure 1.1 below shows the 8-vertex triangulations $\tau(46666677)$ and $\tau(66666666)$. We are naming these particular triangulations by their degree sequence. In each of these two cases, the degree sequence determines the combinatorial type.

*Supported by N.S.F. Research Grant DMS-2505281

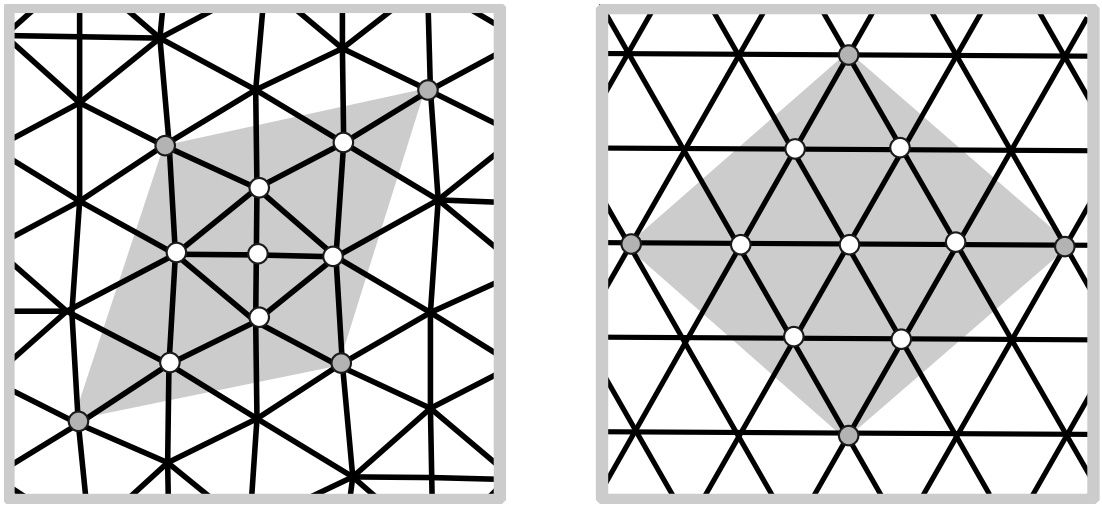


Figure 1.1: The triangulations $\tau(46666677)$ and $\tau(66666666)$.

An *origami torus* is an embedded topological torus in $\boldsymbol{R}^3$ that is made by fitting together finitely many triangles so that the cone angle around each vertex is 2π. Equivalently, an origami torus is the image of a piecewise affine isometric embedding $\phi : T \to \boldsymbol{R}^3$ of a flat torus T. This is to say that T has a triangulation τ such that the restriction of ϕ to each triangle of τ is an isometric affine map. (The specific triangulation is part of the data.) We call a lattice Λ *realized* by τ if there exists an origami torus associated to the lattice Λ and the combinatorial type τ. We call a combinatorial type τ *universal* if every lattice Λ is realized by τ. Here is our main result.

Theorem 1.1 (Universality) $\tau(46666677)$ *is universal.*

The Universality Theorem says that there is a single 8-vertex combinatorial type out of which you can build an origami torus of any shape you like. Our construction yields 2 continuous families of 8-vertex origami tori based on $\tau(46666677)$ which together realize all shapes. We do not know if a single continuous family suffices. Here 8 is as good as it gets: In [**S1**] it is proved that 7-vertex origami tori do not exist. See also [**S2**].

1.2 History and Context

The Universality Theorem is the culmination of a series of results about origami tori, some quite recent.

• In 1960, Y. Burago and V. Zalgaller [**BZ1**] give the first construction of origami tori. In their subsequent 1995 paper [**BZ2**], they prove that one can realize every isometry class of flat torus as an origami torus. In the language above, we would say that every lattice is realized by some combinatorial type.

• The works of T. Tsuboi [**T**] and (independently) P. Arnoux, S. Lelièvre, and A. Málaga [**ALM**] give an explicit construction which realizes every lattice. Both works realize every lattice using the origami tori known as *diplotori* [1] and first described by U. Brehm [**Br**] in 1978. See also the description of these tori in H. Segerman's book [**Se**, §6]. These constructions require infinitely many different combinatorial types.

• The 2024 paper of F. Lazarus and F. Tallerie [**LT**] gives a universal triangulation having 1217 vertices. This paper also has an excellent discussion of the various attempts made to realize all lattices as origami tori.

• In [**S1**], R.E.S. constructed an 8-vertex origami torus and proved that a 7-vertex origami torus does not exist. See also [**S2**]. The 8-vertex origami tori in [**S1**] and [**S2**], called *pup tents*, have combinatorial type $\tau(66666666)$ and are symmetric with respect to order 2 rotation about the Z-axis.

• In [**DS**], P.G.D. and R.E.S. prove that a lattice is realized by a pup tent provided that it is neither rectangular nor sharp rhombic. A lattice is *rectangular* if it is generated by a pair of perpendicular vectors and *sharp rhombic* if it is generated by a pair of equal-length vectors which make an angle of at most $\pi/3$ with each other. When the angle is $\pi/3$ you get the famous *hexagonal lattice*. Thus, almost every lattice is realized by a pup tent. In [**DS**] the authors speculate that perhaps the remaining lattices can be realized by 8-vertex origami tori without 2-fold symmetry.

• In the 2026 paper [**L**], F. Lander proves that the square lattice is realized by $\tau(66666666)$ and the hex lattice is realized by $\tau(46666677)$.

The result in [**L**] grew out of some experiments that F.L. and S.T. did in the summer of 2026. These authors made a poster for R.E.S.'s birthday conference and, in an exciting development, their software could realize some rectangular and sharp rhombic lattices. Upon further experimentation, F.L. and S.T. discovered that the folding pattern used to realize the hexagonal lattice from $\tau(46666677)$ turned out to be extremely robust. This fact led to the Universality Theorem.

[1] For the rectangular lattices one needs a slightly modified construction.

1.3 Proof Strategy and Philosophy

If we fix a triangulation τ, the set $O(\tau)$ of all origami tori which have τ as the underlying combinatorial type is a semi-algebraic set. This is to say that $O(\tau)$ is cut out by algebraic equalities and inequalities. The equalities govern the intrinsic flatness conditions – i.e. the 2π angle sum – around each vertex, and the inequalities govern the embedding property.

Here is how this works. The variables are

1. A point (x, y) such that Λ is generated by $(1, 0)$ and (x, y).

2. A collection of 8 points $w_0, ..., w_7 \in \boldsymbol{R}^2$.

3. Points $p_0, ..., p_7 \in \boldsymbol{R}^3$ realizing the vertices of a member of $O(\tau)$.

The equalities mentioned above say that each relevant distance $\|p_i - p_j\|^2$ equals an expression of the form $\|w_i' - w_j'\|^2$ where w_i' and w_j' are suitable Λ-translates of w_i and w_j, chosen so that the segment joining w_i' and w_j' is isometric to the corresponding edge of τ. Various polynomial inequalities, encoding the positions of the triangles in space, determine the embedding properties.

Ideally, we would like to get explicit coordinates for the vertices of points in $O(\tau)$. This seems quite difficult, partly because there are too many choices to make. The central idea that emerged in [**DS**] is that one should try to parametrize points in the boundary $\partial O(\tau)$. This boundary is a stratified space, and the points in it correspond to *gracefully immersed origami tori*. Such an object is a piecewise affine isometric map $\phi : T \to \boldsymbol{R}^3$ which is not an embedding but which is approximated arbitrarily closely by piecewise affine isometric embeddings.

Essentially, when we move to the boundary we allow certain faces to collapse together. Roughly speaking, the more we have collapsed the faces, the lower the dimension of the stratum we land in. For gracefully immersed origami tori, the map ϕ is very important because it records how the collapsing is done.

The collapsing operation makes certain choices for us, and gives us a better chance of finding nice parametrizations of boundary strata. In [**DS**], the authors found a 2-dimensional stratum which was essentially a copy of a fundamental domain for the modular surface, the hyperbolic orbifold that parametrizes lattices modulo similarity. Aside from one square root, the parametrization is rational. Once the authors found this parametrization, they found an algebraic path from the boundary stratum back into $O(\tau)$. Certain degeneracies prevented the path from realizing rectangular and sharp rhombic lattices. The strategy here is similar but we get everything.

Step 1: In the present setting, where we work with $\tau = \tau(46666677)$, we give an explicit rational parametrization of a 5-dimensional boundary stratum. This stratum is very special: The corresponding gracefully immersed origami tori lie entirely in the plane! This is the first step of our construction. We call these origami tori *flattened origami tori*. We will give formulas in §3.

Step 2: We think of our origami tori as living in $\boldsymbol{R}^2 \times \{0\}$. Once we have parametrized our flattened origami tori, we will establish (to a sufficient extent) that they have a certain *lifting property*. This means that we will keep the XY-coordinates the same and add suitable Z-coordinates $(tz_0, ..., tz_7)$, depending on the example, so that the flattened origami torus becomes an embedded polyhedral torus. This embedded polyhedral torus will not quite be flat; its angle sums will equal 2π up to an error of $O(t^2)$. At the same time, the relevant quantities whose positivity certifies embeddedness will increase from 0 at a rate that is linear in t. In other words, this purely vertical lifting fixes the embedding problem at a much faster rate than it messes up the flatness property. What we mean by *to a sufficient extent* is that we will not establish this lifting property for the full 5-dimensional family, but only for a 2-dimensional subset which is sufficient to realize every similarity class of lattice. We carry this out in §4.

Step 3: Our lifting path does not quite give us origami tori on the nose. To correct the lifting path, we will use a strategy similar to what is done in [**DS**]. We prove a transversality result, essentially the Implicit Function Theorem, which shows that we can recover perfect flatness by an $O(t^2)$ perturbation of the coordinates – a perturbation that is too small to mess up the embedding property. An easy topological degree argument finishes the proof. We do all this in §5.

1.4 Organization

In §2 we will have a short section on algebraic material which will greatly help with our proofs. This material may not seem closely related to the Universality Theorem at first, but in §3-5 the connection will become apparent. The main thrust of the material in §2 is to explain how we treat rational functions on the so-called modular domain in a uniform algebraic way.

Following the preliminary material in §2 we get to the main steps described above.

1.5 Computer Calculations

We perform our calculations in Mathematica [**W**]. These calculations are all fairly short and easy to reproduce. One file contains everything:
http://www.math.brown.edu∼res/Java/UniversalityProof

1.6 Artificial Intelligence Use

We used Artificial Intelligence in a moderate way. The conceptual framework for the proof is ours, and evolved from the papers [**S1**], [**DS**], and [**L**]. At various stages, ChatGPT 5.6 implemented some of our search algorithms and optimized some of our code. Perhaps needless to say, the AI also helped format equations, provide references, and proofread the paper. Also, we mention that ChatGPT had an excellent idea for simplifying the angle-derivative formulas for the Jacobian calculation in §4.

1.7 Acknowledgements

R.E.S. would like to thank the I.H.E.S for their support, in the form of the Gretchen and Barry Mazur Chair, during the writing of this paper.

2 Preliminaries

2.1 Rational Parametrization of Circular Arcs

We call a function $f : \boldsymbol{R}^2 \to \boldsymbol{R}$ *fully rational* if it is a rational function with rational coefficients. All functions we deal with in this paper will be fully rational. We will often abbreviate this by saying that f is *rational*.

Let C denote the arc of the unit circle $x^2 + y^2 = 1$ with $x, y \geq 0$. We have the following rational parametrization $\psi : [0, 1] \to C$ given by

$$x = \frac{2t}{1+t^2}, \qquad y = \frac{1-t^2}{1+t^2}. \tag{1}$$

If we have a rational function $f : \boldsymbol{R}^2 \to \boldsymbol{R}$ and we want to certify that f does not vanish on C, it suffices to show that the composition $f_* = f \circ \psi$, another rational function, does not vanish on $[0, 1]$. Taking numerators and fixing the sign, we reduce to the problem of showing that an integer polynomial is positive on $[0, 1]$. This little situation is a toy model for what we do more generally in the paper.

To make this approach more flexible, let $x_0, x_1 \in \boldsymbol{R} \cap [0,1]$. Let $C|_{[x_0,x_1]}$ denote the sub-arc of C where $x \in [x_0, x_1]$. We choose $r_0, r_1 \in \boldsymbol{Q} \cap [0,1]$ such that

$$\frac{2r_0}{1+r_0^2} \le x_0 < x_1 \le \frac{2r_1}{1+r_1^2}. \tag{2}$$

We then define

$$\psi_*(t) = \psi(t_*), \qquad t_* = (1-t)r_0 + (t)r_1. \tag{3}$$

Then $\psi_*([0,1])$ is an arc that contains $C|_{[x_0,x_1]}$. To prove that f does not vanish on $C|_{[x_0,x_1]}$ it suffices to show that $f \circ \psi_*$ does not vanish on $[0,1]$.

2.2 The Modular Domain

Using the notation from above, let

$$\mathcal{M}|_{[x_0,x_1]} = \left\{(x, y+h) : \ (x,y) \in C|_{[x_0,x_1]}, \ \ h \ge 0\right\}. \tag{4}$$

In particular, let

$$\mathcal{M} = \mathcal{M}|_{[0,1/2]}. \tag{5}$$

We think of $\mathcal{M}$ as a subset of $\boldsymbol{H}^2$, the upper half-plane model of the hyperbolic plane. The subset $\mathcal{M}$ is the fundamental domain for the action of the $(2,3,\infty)$ reflection triangle group, a group which contains the modular group $PSL_2(\boldsymbol{Z})$ with index 2. Up to scaling and reflection, every lattice is parametrized by a point in $\mathcal{M}$. Abusing terminology slightly, we call $\mathcal{M}$ the *modular domain*.

We will parametrize a superset of $\mathcal{M}|_{[x_0,x_1]}$ by two unit squares, in the following way. We let ψ_* be as in Equation 3. We then define

$$F_A(t,h) = \psi_*(t) + (0,h), \qquad F_B(t,h) = \psi_*(t) + (0,1/h). \tag{6}$$

The domain for F_A is $Q_A := [0,1] \times [0,1]$. The domain for F_B is $Q_B := [0,1] \times (0,1]$; the lower edge is missing in this case. By construction,

$$\mathcal{M}|_{[x_0,x_1]} \subset F_A(Q_A) \cup F_B(Q_B). \tag{7}$$

To prove that a rational function $f : \boldsymbol{R}^2 \to \boldsymbol{R}$ does not vanish on $\mathcal{M}|_{[x_0,x_1]}$ it suffices to prove that $f \circ F_A$ and $f \circ F_B$ do not vanish respectively on Q_A and Q_B.

Remark: We are using the convention that a rational function is defined even when it has poles, but in our situation every rational function in sight will be finite on the domains of interest.

2.3 Preprocessing

We want to prove that various rational functions do not vanish on Q_A or on Q_B, as the case may be. In this section we present two tricks which reduce this to a problem of showing that an integer polynomial is positive on $Q_A = [0,1]^2$. We call these tricks *preprocessing*.

Clearing Denominators: Let $R = P/Q$ be a rational function on $\boldsymbol{R}^2$. We can write this expression so that P is an integer polynomial with $P(1/2, 1/2) \geq 0$ and P, Q have no common factors. If R is finite on $[0,1]^2$ and $P > 0$ on $[0,1]^2$ then neither R nor Q vanishes on $[0,1]^2$. So we can work with P rather than R.

Factoring Out the Height: For the test on the domain Q_B, we write

$$P(t,h) = h^k P^*(t,h),$$

where P^* is another polynomial and $k \geq 0$ is as large as possible. Showing that $P^* > 0$ on $[0,1]^2$ is the same as showing that $P > 0$ on Q_B. We work with P^*.

2.4 Positive Dominance

After preprocessing our various functions, we are left with proving that a polynomial is positive on the unit square $[0,1]^2$. In this section we explain how we do it. This material is adapted from [**S3**].

We start with a warm-up problem. Given a polynomial $P(x) = a_0 + a_1 x + ... + a_n x^n$ define $A_k = a_0 + ... + a_k$. We say that P is *positive dominant* if all $A_k > 0$ for all k.

Lemma 2.1 *If P is positive dominant then $P > 0$ on $[0,1]$.*

Proof: If $n = 0$ or if $x = 0$ the result is obvious. Let $x \in (0,1]$. Since $a_0 \geq a_0 x$, we have

$$P(x) \geq A_1 x + a_2 x^2 + ... + a_n x^n = xQ(x) > 0.$$

The final inequality comes from the fact that $Q(x)$ is again positive dominant and from induction on the degree. ♠

Now we consider a 2 variable version of this. Let $P \in \boldsymbol{R}[x_1, x_2]$ be a two-variable polynomial. (In practice we will have $P \in \boldsymbol{Z}[x_1, x_2]$.) We can write

$$P = \sum_I c_I X^I, \qquad X^I = \prod_{i=1}^2 x_i^{I_i}. \tag{8}$$

Here each I has the form (I_1, I_2). Given two multi-indices I and J, we write $I \preceq J$ if $I_i \leq J_i$ for $i = 1, 2$. Define

$$\Sigma_J = \sum_{I \preceq J} c_I. \tag{9}$$

We call P *positive dominant* if $\Sigma_J > 0$ for all J.

Lemma 2.2 *If P is positive dominant, then $P > 0$ on $[0,1]^2$.*

Proof: Let $P = f_0 + f_1 x_2 + \cdots + f_m x_2^m$, where $f_0, ..., f_m$ are single-variable polynomials in x_1. Each single variable polynomial

$$P_j = f_0 + \cdots + f_j$$

is positive dominant. By the single-variable result, $P_j > 0$ on $[0,1]$. Now fix $x_1 \in [0,1]$ and consider $Q(x_2) = P(x_1, x_2)$. Here $Q(x_2)$ has successive partial sums $A_j = P_j(x_1) > 0$ for $j = 0, ..., m$. Hence $Q > 0$ on $[0,1]$ by the single-variable case. ♠

Tweaks: Let $\widetilde{P}(t,h) = P(1-t,h)$. If $\widetilde{P}$ is positive dominant then $P > 0$ on $[0,1]^2$. More generally, if $Y \subset [0,1]^2$ is a rational axis-aligned sub-square then we can show that $P|_Y$ is positive by choosing an affine map $A : [0,1]^2 \to Y$ and then showing that $P|_Y \circ A$ is positive dominant. This fact suggests a recursive subdivision algorithm that halts with success if and only if $P > 0$ on $[0,1]^2$. We don't need this algorithm for the present work.

2.5 Summary

Suppose we have a fully rational function $f : \boldsymbol{R}^2 \to \boldsymbol{R}$ and we want to show that f does not vanish on $\mathcal{M}|_{[x_0,x_1]}$.

1. We choose r_0, r_1 as in Equation 2.
2. We define rational parametrizations $F_A : Q_A \to \boldsymbol{R}^2$ and $F_B : Q_B \to \boldsymbol{R}^2$ such that $\mathcal{M}|_{[x_0,x_1]} \subset F_A(Q_A) \cup F_B(Q_B)$.
3. We preprocess $f \circ F_A$ and $f \circ F_B$ and get integer polynomials P_A and P_B^*.
4. We use the Mathematica file **UniversalityProof** to show that P_A and P_B^* are positive dominant, and hence positive on $[0,1]^2$.

Tweaked Method: In one case (Lemma 5.1) we show instead that $\widetilde{P}_A$ and P_B^* are positive dominant.

3 The Flattened Tori

3.1 The 5 Parameter Family

We are going to describe a 5-parameter family of flattened origami tori. We think of this family as a fiber bundle over a base space coordinatized by (x, y). The fiber is parametrized by variables (u, k, λ) which satisfy certain algebraic constraints.

The Lattice: The variables (x, y) correspond to a lattice

$$\Lambda = \boldsymbol{Z}(1, 0) + \boldsymbol{Z}(x, y). \tag{10}$$

That is, Λ is the $\boldsymbol{Z}$-lattice generated by $(1, 0)$ and (x, y). Here we are suppressing the dependence of Λ on x and y.

The Parameters: The base space [2] will be $\mathcal{M}$, the modular domain from Equation 5. Here are the constraints on the fiber (u, k, λ).

$$u, k, \lambda/2, x + k - u \in (0, 1/2).$$

$$u < \frac{\lambda(1-\lambda)C + \lambda(x + k - 1/2)}{\lambda + 2k(1-\lambda)}, \qquad C = (1-x)(1-2k) + 2k^2. \tag{11}$$

Remarks: These constraints are hard to understand, but we will never actually need to use them. Rather, we will present explicit 2-parameter subfamilies and then directly check that they have the needed properties. The complicated algebraic nature of the constraints reflects some beautiful geometry behind these families.

The Flattened Origami Torus: Here are the points of the corresponding flattened torus $T(x, y, u, k, \lambda)$. Again, we will simplify this unwieldy expression by taking explicit choices for u, k, λ as functions of x and y.

[2] The entire base space for the family is larger, but we only care about this subset.

$$
\begin{aligned}
p_0 &= (0,0,0),\\
p_1 &= \left(u,\ \frac{u(\lambda(1-x-2k)+2k)}{\lambda y},\ 0\right),\\
p_2 &= \left(u-\frac{1}{2},\ \frac{x(1/2-u)}{y},\ 0\right),\\
p_3 &= \left(-k-\lambda(1-x-2k),\ \frac{\lambda(y^2-(1-x-2k)^2)-2k(1-x-2k)}{2y},\ 0\right),\\
p_4 &= \left(x+k-\frac{1}{2},\ \frac{y^2+x(1-x-2k)}{2y},\ 0\right),\\
p_5 &= \left(u-\frac{1}{2},\ \frac{y^2+2(1-x-2k)(u-k-x/2)}{2y},\ 0\right),\\
p_6 &= \left(u-k,\ \frac{(1-x-2k)(u-k)}{y},\ 0\right),\\
p_7 &= \left(u,\ \frac{u(1-x-2k)+\frac{1}{2}((1-x-2k)^2+y^2)-\frac{u-x-k+1/2}{1-\lambda}}{y},\ 0\right).
\end{aligned}
$$

The Flat Torus: We will describe 16 triangles. We get a tiling of $\boldsymbol{R}^2$ by taking the orbit of these triangles under the action of the lattice Λ defined above. The quotient then gives us our 8 vertex triangulation of $\boldsymbol{R}^2/\Lambda$. Here are the triangles

$$
\begin{array}{llll}
012 & (w_0,w_1,w_2) & 167 & (w_1,w_6,w_7)\\
031 & (w_0,w_3,w_1) & 264 & (w_2+e,w_6,w_4+e-\tau)\\
024 & (w_0,w_2,w_4-\tau) & 257 & (w_2+e,w_5+e,w_7)\\
043 & (w_0,w_4-\tau,w_3) & 276 & (w_2+e,w_7,w_6)\\
152 & (w_1,w_5,w_2) & 347 & (w_3+\tau,w_4,w_7)\\
136 & (w_1,w_3,w_6) & 356 & (w_3,w_5+e-\tau,w_6)\\
145 & (w_1,w_4,w_5) & 375 & (w_3+\tau,w_7,w_5+e)\\
174 & (w_1,w_7,w_4) & 465 & (w_4+e-\tau,w_6,w_5+e-\tau)
\end{array}
\tag{12}
$$

Here $e=(1,0)$ and $\tau=(x,y)$. The points $w_0,...,w_7$ are the same as $p_0,...,p_7$,

except for w_3 and w_6:

$$w_3 = \left(k, -\frac{2k(1-x-2k)+\lambda((1-x-2k)^2+y^2)}{2y}\right),$$

$$w_6 = \left(u+k, \frac{(1-x-2k)(u-k)}{y}\right).$$

Preliminary Isometric Mapping: Let W_k denote the kth triangle above. We call the set $\{W_0, ..., W_{15}\}$ the *fundamental triangles*. Let P_k denote the corresponding triangle whose vertices are the p_i.

Lemma 3.1 *The affine map $W_k \to P_k$ is an isometry for $k = 0, ..., 15$.*

Proof: We compute this exactly with the file **Universality Proof**. ♠

3.2 The Special Families

Here are the parameter choices for the two special families.

$$\text{Family 1}: \quad u = \frac{3}{128}, \quad k = \frac{11}{32}, \quad \lambda = \frac{13}{32}.$$

$$\text{Family 2}: \quad u = \frac{x}{2} - \frac{1}{2048}, \quad k = \frac{1}{16}, \quad \lambda = \frac{1}{2}.$$

We are interested in the first family for $x \in [0, x_0]$ and in the second family for $x \in [x_0, 1/2]$. Here

$$x_0 = u(\frac{5}{64}) = \frac{640}{4121} = .1553..., \qquad u(t) = \frac{2t}{t^2+1}.$$

With these restrictions, the constraints above are satisfied. However, we do not need to check this. There is some amount of leeway in our choice of x_0 but the tolerance is small. When we use the method in §2.5 we always do this:

1. We take $r_0 = 0$ and $r_1 = 5/64$ for the first family.
2. We take $r_0 = 5/64$ and $r_1 = 9/32$ for the second family.

In the second case we have $u(9/32) > 1/2$, so our choice works.

Pictures: Figure 3.1 shows the triangulated flat torus associated to the parameters $(x, y) = (0, 1)$, the square lattice. This is in the first family.

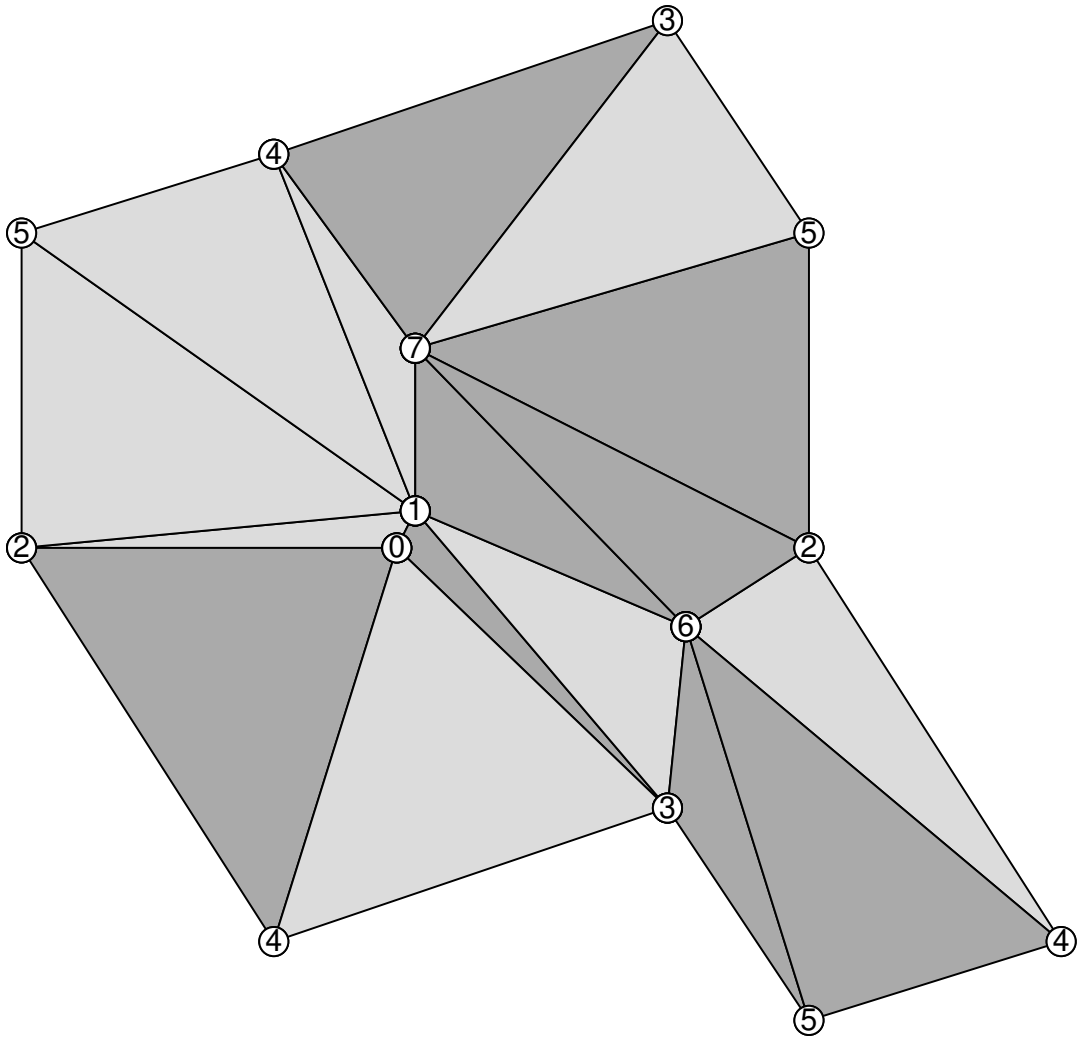


Figure 3.1: The triangulated flat torus associated the square lattice.

From the vertex labeling you can see how the action of Λ identifies the edges along the boundary to make the torus. We have shaded the triangles to indicate whether the map from these triangles to the flattened origami torus preserves or reverses orientation. Up to a global sign, the binary sequence 0110000010111101 carries all the information about the orientations.

Figure 3.2 shows the origami torus built triangle by triangle. The ordering of the faces is compatible with the ordering coming from the lift we construct in §4.

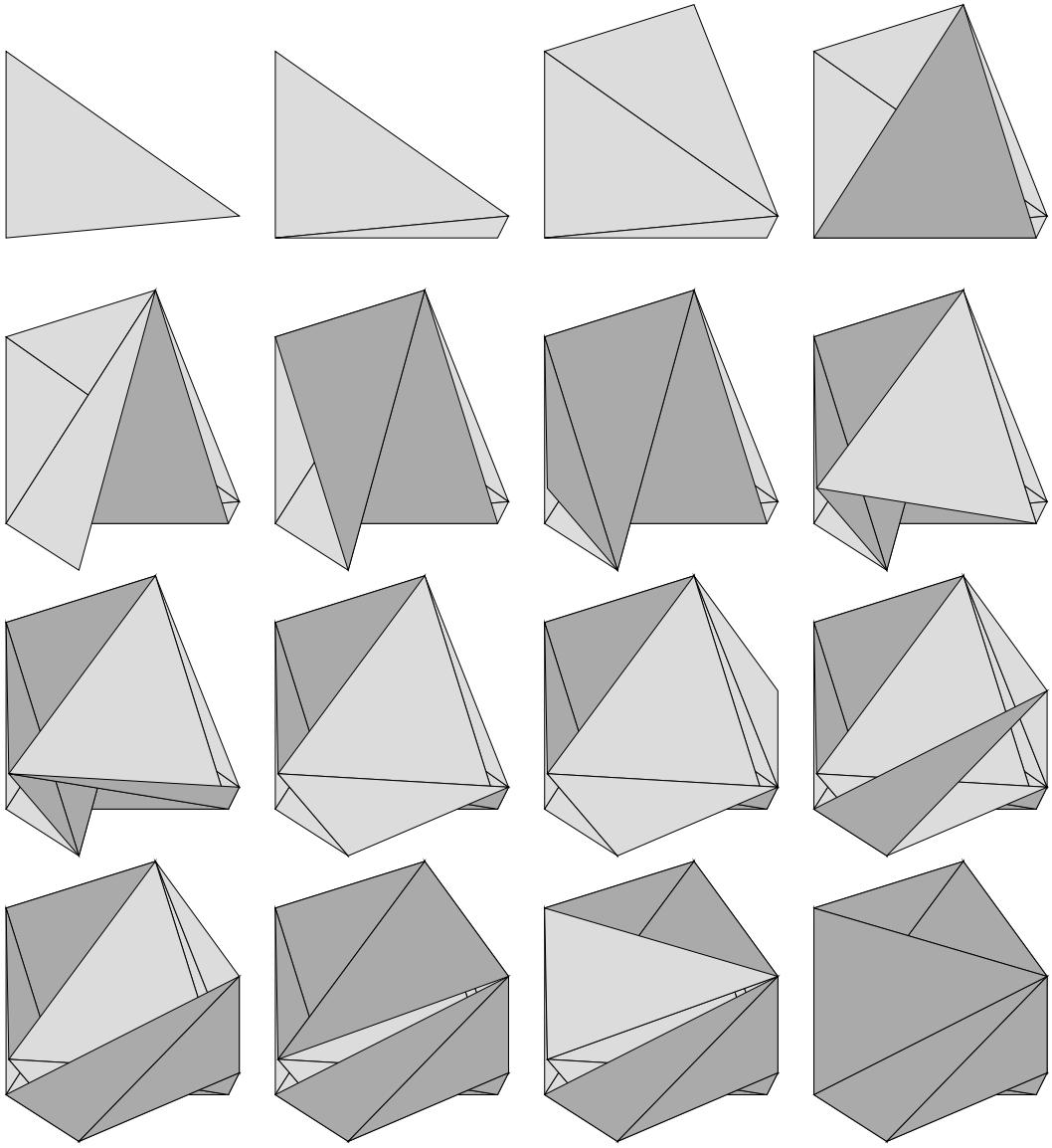


Figure 3.2: The flattened origami torus associated to the square lattice.

Figures 3.3 and 3.4 show the same thing as for the parameter $(8/17, 1)$. This is in the second family. A more natural choice would be the parameter $(1/2, \sqrt{3}/2)$ for the hex lattice, but in this case the picture does not look great. Two of the points are very close together for the hex lattice picture.

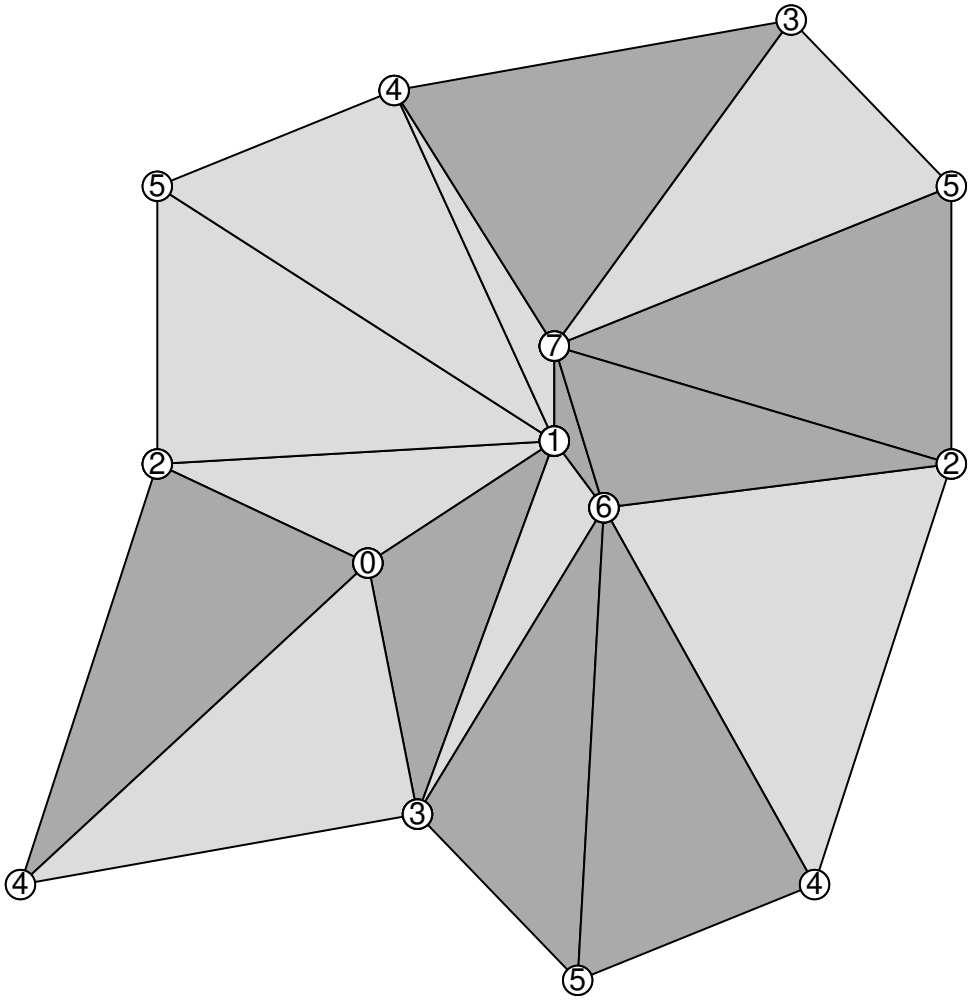


Figure 3.3: The triangulated flat torus associated to $(8/17, 1)$.

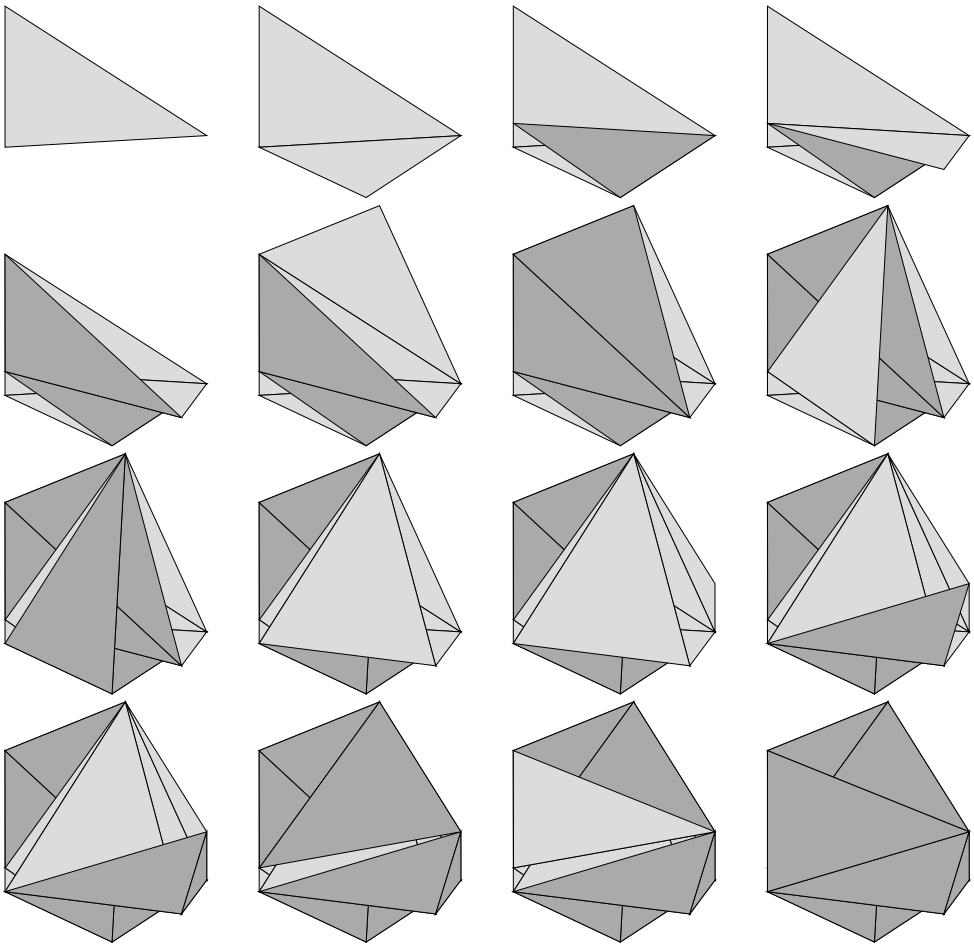


Figure 3.4: The flattened origami torus associated to $(8/17, 1)$.

3.3 The Fundamental Domain Lemma

For each family we have 16 continuously varying fundamental triangles.

Lemma 3.2 *For each family and for every parameter, every fundamental triangle has positive area.*

Proof: Each triangle T has vertices A, B, C which are rational functions of the variables t, h. We compute the rational function $\det(A - C, B - C)$ and then certify their nonvanishing using the method summarized in §2.5. ♠

Lemma 3.3 (Fundamental Domain) *For each parameter of each family the union F of fundamental triangles is a fundamental domain for the action of Λ, and the quotient F/Λ is isometric to $\mathbf{R}^2/\Lambda$.*

Proof: Our proof uses the familiar property that in a connected topological space X, a nonempty subset $S \subset X$ equals X provided that S is open and closed.

Consider the first family. Let $X = \mathcal{M}_{[0,x_0]}$ be the domain for the first family. Let $S \subset X$ denote the set of parameters for which the Fundamental Domain Lemma is true. Given the combinatorial action of Λ on the fundamental triangles, S is an open set. Lemma 3.2 implies that S is closed because the fundamental triangles cannot degenerate at any point of X. Looking at the pattern of triangles in Equation 12 and comparing it with Figure 3.1, we see that S contains the point $(0,1)$. This is a crude check which just involves the rough positions and orientations of the triangles. Hence $S = X$.

The analysis of the second family works the same way, using Figure 3.3 in place of Figure 3.1.

Finally, the non-degeneracy of the triangles is sufficient to prove this lemma because their orientations are constant throughout each family. Thus, no overlaps can develop as we move around in the parameter space. ♠

The Fundamental Domain Lemma lets us promote our folding map to a flattened origami torus $\phi : \mathbf{R}^2/\Lambda \to \mathbf{R}^2$. The point is that our map respects the side identifications on the fundamental domain made from the union of the 16 fundamental triangles.

4 The Lifting Property

4.1 The Main Result

We think of $\mathbf{R}^2$ as the subset $\mathbf{R}^2 \times \{0\} \subset \mathbf{R}^3$. Let $\pi : \mathbf{R}^3 \to \mathbf{R}^2$ be the projection map. Let $\phi : T \to \mathbf{R}^2$ be a flattened origami torus. We say that a *lift* of ϕ is a piecewise affine embedding $\widehat{\phi} : T \to \mathbf{R}^3$ such that $\pi \circ \widehat{\phi} = \phi$.

The data for a lift simply amounts to choosing a list $(z_0, ..., z_7)$ of third coordinates for the 8 vertices of $\phi(T)$. Here is our lift for Family 1.

$$0 \quad 0 \quad -2 \quad 3 \quad 1 \quad -2 \quad 2 \quad 1024 + 1024y^2 \tag{13}$$

Here is our lift for Family 2.

$$0 \quad 0 \quad -4 \quad -2 \quad 2048 \quad -4 \quad 1816x - 229 \quad 16384 + 16384y^2 \tag{14}$$

In this chapter we will prove that these really are lifts: The resulting polyhedral tori are embedded.

Remark: We found these by trial and error. They are really delicate. For instance, if you replace 229 by either 228 or 230 the resulting lift does not work.

4.2 General Position

We call a polyhedral torus *flexed* if its points are in general position. This means that no 4 vertices are coplanar.

Lemma 4.1 *For both special families, every lifted polyhedral torus is flexed.*

Proof: For each quadruple $q = a, b, c, d$ and each special family we compute

$$\det(p_a - p_d, p_b - p_d, p_c - p_d) \tag{15}$$

We then certify nonvanishing for each of the 140 rational functions using the method summarized in §2.5. ♠

4.3 The Embedding Test

Let T be one of our triangulated flat tori. Let $\mathcal{T}$ be the triangulation. Let $f : T \to \boldsymbol{R}^3$ be a piecewise affine map. We assume that f is injective on each triangle separately and that f maps the vertices of $\mathcal{T}$ to points in general position.

Lemma 4.2 *Suppose that $f(e) \cap f(\tau) = \emptyset$ provided that e is an edge of $\mathcal{T}$ and τ is a triangle of $\mathcal{T}$ and $e \cap \tau = \emptyset$. Then f is an embedding.*

Proof: It suffices to establish the following stronger property: for every pair τ_1, τ_2 of triangles of $\mathcal{T}$,

$$f(\tau_1) \cap f(\tau_2) = f(\tau_1 \cap \tau_2). \tag{16}$$

Suppose that f is not an embedding. Then Equation 16 fails for some pair τ_1, τ_2 of triangles. There are three cases.

1. Suppose τ_1 and τ_2 share an edge. If Equation 16 fails for this pair, then the 4 vertices of $f(\tau_1) \cup f(\tau_2)$ would be coplanar. This is a contradiction.

2. Suppose that $\tau_1 \cap \tau_2 = \emptyset$. If $f(\tau_1)$ intersects $f(\tau_2)$ then some edge of one of these triangles intersects the other triangle.

3. Suppose that τ_1 and τ_2 have exactly one vertex v in common. If $f(\tau_1)$ and $f(\tau_2)$ are coplanar we have the same contradiction as in Case 1. Otherwise, since Equation 16 fails for this pair, $f(\tau_1) \cap f(\tau_2)$ is a line segment connecting $f(v)$ to some point w. There is an index j so that $w \in f(\tau_j)$ and w lies in the edge of $f(\tau_{3-j})$ opposite $f(v)$. This is a contradiction.

All cases work out. ♠

Remark: The above criterion works even if we do not assume that f maps the vertices of $\mathcal{T}$ to points in general position. We leave this to the interested reader.

Now we turn to the question of how we tell when a line segment $(A_0, A_1) \subset \boldsymbol{R}^3$ is disjoint from a triangle $(A_2, A_3, A_4) \subset \boldsymbol{R}^3$. We treat the case when these points are in general position because that is all we need. Here we are naming these objects by their vertices. If we delete A_k from the list we get a tetrahedron T_k, and we let V_k denote the volume of T_k. To be precise, we put the points of T_k in increasing order and then take the signed volume. The sign counts the orientation.

Lemma 4.3 (01) *and* (234) *are disjoint provided* $\max(V_0V_1, V_2V_3, V_3V_4) > 0$.

Proof: Let $[abcd]$ denote the signed volume of the tetrahedron with vertices listed in the order a, b, c, d. If $V_1 = [0234]$ and $V_0 = [1234]$ have the same sign then (01) lies strictly on one side of the plane containing (234). This gives disjointness. If (01) intersects (234) then the three volumes (0123) and (0134) and (0142) have the same sign. This fails if $V_2V_3 > 0$ or $V_3V_4 > 0$. ♠

It turns out that there are 138 pairs (e, τ) where e is an edge of $\mathcal{T}$ and τ is a triangle of T and $e \cap \tau = \emptyset$. We get a proof that T is embedded if all 138 pairs satisfy the criterion above. Using the file **UniversalityProof** we check this for $(0, 1)$ in Family 1 and for $(8/17, 1)$ in Family 2. Since none of the relevant signs changes throughout the families, the same inequalities hold everywhere. Hence, in both families, all lifted polyhedral tori are embedded.

5 The Mapping Result

5.1 The Main Calculation

In this chapter we prove the transversality result that finishes the proof of the Main Theorem.

Let $\phi : T \to \Psi \subset \boldsymbol{R}^2 \times \{0\}$ be one of our flattened origami tori. We set $\Psi = \phi(T)$. Given a 7-vector $\epsilon = (\epsilon_0, ..., \epsilon_6) \in \boldsymbol{R}^7$ let $\Psi(\epsilon)$ be the result of replacing the vertex (x_i, y_i) of Ψ by $(x_i + \epsilon_i, y_i)$. We do not touch vertex 7, the last vertex. We let $\theta = (\theta_0, ..., \theta_6)$ denote the 7-vector of cone angles of the perturbed triangulated torus $\Psi(\epsilon)$. We do not consider the last cone angle θ_7.

For both families we have the Jacobian

$$J = \det \left. \frac{\partial \theta}{\partial \epsilon} \right|_{\epsilon=0}. \tag{17}$$

In other words, we take the 7×7 matrix of partial derivatives of the function $\epsilon \to \theta$ and then we take the determinant.

Lemma 5.1 *For both families, J is nonvanishing on its domain of definition.*

Proof: For each family we use the tweaked method from §2.5 to certify this. (The regular method also works for the first family.) ♠

Remark: Our Jacobian calculation is straightforward except for one fine point which we discuss. The formula for the angle α between two vectors $V = (v_1, v_2)$ and $W = (w_1, w_2)$ is

$$\alpha = \arccos\left(\frac{V.W}{\|V\|\|W\|}\right).$$

This formula is far from rational, but for the derivatives we have e.g.

$$\frac{\partial \alpha}{\partial v_1} = \sigma \frac{v_2}{v_1^2 + v_2^2}, \qquad \sigma = \text{sign}(\det(V, W)).$$

Here is the crucial observation. Since the triangles in our families are non-degenerate everywhere, we can determine all the σ values once and for all by looking at a single example. Both families have the same sequence of signs, so we only need to make one check. This gives us fairly simple rational expressions for J in both cases.

5.2 Lengthening a Segment

Here we discuss a geometric fact that helps with our proof. Let $S \subset \boldsymbol{R}^2 \times \{0\}$ be a line segment of unit length. Suppose that the endpoints of S are $(0,0,0)$ and $(1,0,0)$. How long is the segment with endpoints $(0,0,0)$ and $(1,0,t)$? By the Pythagorean Theorem, the length is $\sqrt{1+t^2} \leq 1+t^2$. This is not the best estimate, of course, but it suffices for our purposes.

The estimate (and scaling) implies that if we consider a path of lifts of a line segment into $\boldsymbol{R}^3$ by a change of height that is linear in t, then the length grows on the order of $O(t^2)$. Let us apply this principle to the lifts of our flattened origami tori. Given a flattened origami torus $\phi : T \to \boldsymbol{R}^2 \times \{0\}$ we constructed an embedded lift $\widehat{\phi}_t : T \to \boldsymbol{R}^3$ in which the heights change linearly with t. The edge lengths of the image $\widehat{\Psi}_t = \widehat{\phi}_t(T)$ change by $O(t^2)$ along this path.

The image $\widehat{\Psi}_t$ is an embedded polyhedral torus. It is not quite an origami torus but it is very close. Let θ_t denote the 8-tuple of angles of $\widehat{\Psi}_t$. By elementary Euclidean geometry – e.g. the Law of Cosines the components of θ_t vary by $O(t^2)$. As we mentioned in the previous chapter, $\widehat{\Psi}_t$ becomes embedded at a linear rate whereas it loses the flatness property at the much slower rate of $O(t^2)$.

5.3 The Pseudo Modulus Function

The polyhedral torus $\widehat{\Psi}_t$ is not in general an origami torus. However, we would still like a way to assign something like a modulus to it in a meaningful way. This *pseudo modulus* should vary smoothly with the vertices and agree with the modulus in case the image is flat. Our construction depends on some choices, but any choices we make are sufficient.

We have been taking our moduli of flat tori to lie in the modular domain $\mathcal{M}$ defined in Equation 5. However (working with complex numbers for convenience) any complex number $\tau \in \boldsymbol{H}^2$ that is $PSL_2(\boldsymbol{Z})$ equivalent to the one in $\mathcal{M}$ would equally well serve as a modulus. Allowing τ to vary in all of $\boldsymbol{H}^2$ is the usual set up we have when we work with Teichmuller space rather than with moduli space.

A *marked flat torus* is a flat torus together with a distinguished basepoint and a distinguished pair of loops L_1, L_2 generating the fundamental group. Since our flat tori come with triangulations which vary continuously within a family, we can choose our markings once and for all so that the distinguished vertex is (say) the point w_0 and the two generating loops are edge paths in the triangulation.

In case we have a piecewise affine map $\phi : T \to \Psi \subset \boldsymbol{R}^3$ we can extract a planar parallelogram, as follows. We first form the space $\widehat{T}$ which is a triangulated

homeomorphic copy of $\boldsymbol{R}^2$ in which each triangle is isometric to the corresponding triangle of Ψ. In general $\widehat{T}$ is an infinite flat cone surface. When Ψ is an origami torus, $\widehat{T}$ is isometric to $\boldsymbol{R}^2$.

Working in $\widehat{T}$, we choose 1-sided combinatorial neighborhoods $\widehat{N}_1$ and $\widehat{N}_2$ respectively of the lifts $\widehat{L}_1$ and $\widehat{L}_2$, as shown on the left side of Figure 5.1. We arrange it so that $\widehat{v}_0 = \widehat{L}_1 \cap \widehat{L}_2$ is incident to a common triangle $\widehat{\Delta} \subset \widehat{N}_1 \cap \widehat{N}_2$.

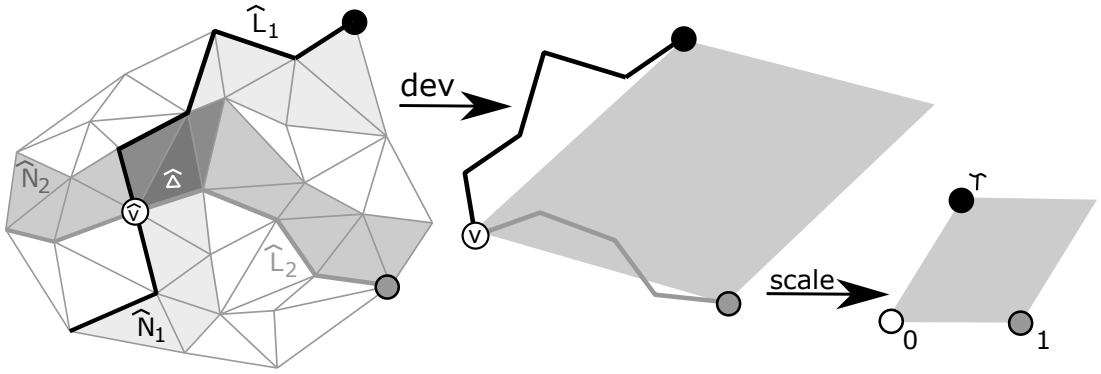


Figure 5.1: The developed parallelogram

We then develop $\widehat{L}_1$ and $\widehat{L}_2$ into the plane using the $\widehat{N}_1$ and $\widehat{N}_2$. We make the image of $\widehat{\Delta}$ the same for both developments.

When we take one period of this development map for each lifted loop, we get a parallelogram, as in the right side of Figure 5.1. We make a consistent choice of $\widehat{N}_1$ and $\widehat{N}_2$ throughout a neighborhood of the point of interest to us, so that τ varies smoothly. If Ψ is flat then τ equals the modulus of Ψ up to $PSL_2(\boldsymbol{Z})$-equivalence.

5.4 The Local Diffeomorphism

Now we make a crucial observation. For any point ζ in either of the two domains, the corresponding special family is defined in an open neighborhood of ζ. All of our positivity results hold by continuity in a sufficiently small open neighborhood $U \subset \boldsymbol{R}^2$ around ζ. We define a map

$$F : \boldsymbol{R}^7 \times \boldsymbol{R} \times U \to \boldsymbol{R}^7 \times \boldsymbol{R} \times \boldsymbol{C}. \tag{18}$$

The variables for the domain are the perturbation vector ϵ discussed above, a real parameter t, and the modulus p of the flat torus.

Now we construct the map F. We let $\widehat{\Psi}_{t,p} = \widehat{\phi}_t(T_p)$ be our lifted polyhedral torus, where we lift by the vector $(tz_0, ..., tz_7)$ of heights. Finally, we perturb the

X-coordinates to get $\widehat{\Psi}_{t,p}(\epsilon)$. This is our X-perturbed lifted polyhedral torus. We define

$$F(\epsilon, t, p) = (\theta, t, \tau) \tag{19}$$

Here τ is the pseudo-modulus of $\widehat{\Psi}_{t,p}(\epsilon)$. Everything in sight varies smoothly. Note that $F(\overrightarrow{0}, 0, p) = (\vartheta, 0, g(p))$ for all $p \in U$. Here $g \in PSL_2(\boldsymbol{Z})$ is some fixed element.

Lemma 5.2 *dF is nonsingular at $(\overrightarrow{0}, 0, \zeta)$.*

Proof: The modulus is a complex parameter which for the purposes of this calculation we identify with a point in $\boldsymbol{R}^2$. Thus dF is a 10×10 matrix. To fix conventions, the columns are what we get by differentiating with respect to a fixed variable. The rows are what we get by differentiating a fixed variable with respect to all the others. We will show that

$$dF = \begin{pmatrix} A & 0 & 0 \\ 0 & 1 & 0 \\ B & 0 & dg \end{pmatrix} \tag{20}$$

Here, the matrix A is the upper 7×7 minor of dF. This is the invertible matrix $\partial\theta/\partial\epsilon$ which we considered in our main calculation, and dg is the differential of $g \in PSL_2(\boldsymbol{Z})$ considered as a real 2×2 (nonsingular) matrix. So, to finish the proof, we just have to establish Equation 20.

We have already discussed the block A in Equation 20. Here is the rest of the analysis.

- We have $\partial\theta/\partial t = 0$ because these angles are changing by $O(t^2)$. At the same time we have $\partial t/\partial v = 0$ for any variable $v \neq t$. Thus, the upper 8×8 minor of dF has block diagonal form with a $1 = \partial t/\partial t$ on the diagonal.
- More strongly, the 8th row, representing $\partial t/\partial v$, has all zeros except for the single 1 we have already mentioned.
- The 8th column has just a single 1. The reason is that $\partial\theta/\partial t = 0$ by construction and $\partial\tau/\partial t = 0$ because all the edge lengths of our triangulation change by $O(t^2)$ and hence so does τ.
- We don't care about the bottom block B. This represents $\partial\tau/\partial\epsilon$.
- We have $\partial\theta/\partial p = 0$ because we are evaluating this entirely on flattened origami tori. This makes the upper right block the 0-matrix.

This completes the proof. ♠

5.5 The End of the Proof

Let $\vartheta = (2\pi, ..., 2\pi)$. This vector has length 7. Consider the point

$$q_t = F^{-1}(\vartheta, t, g(\zeta)). \tag{21}$$

Here we mean to use the local inverse of F guaranteed by the Inverse Function Theorem, not the full pre-image. The polyhedral torus Ψ_t associated to q_t is flat because 7 of its 8 cone angles are 2π. The 8th cone angle is also 2π by the Gauss-Bonnet Theorem.

By construction, the pseudo-modulus of Ψ_t is $g(\zeta)$, which is $PSL_2(\boldsymbol{Z})$ equivalent to ζ. To finish the proof we just have to see that Ψ_t is embedded for sufficiently small $t > 0$.

Our original lift (which keeps $\epsilon = 0$) changes the cone angles by $O(t^2)$. Since F^{-1} is smooth, we have $q_t = (0, t, \zeta) + O(t^2)$. We only need to add a correction of $O(t^2)$ to restore the flatness. Since the various volumes which determine the embedding grow linearly with t, they remain nonzero for $t > 0$ sufficiently small. Hence Ψ_t is embedded for $t > 0$ sufficiently small.

This completes the proof of the Universality Theorem.

6 References

[**ALM**] P. Arnoux, S. Lelièvre, A. Málaga, *Diplotori: a family of polyhedral flat tori.* in preparation

[**Br**] U. Brehm, Oberwolfach report (1978)

[**BZ1**] Y. D. Burago and V. A. Zalgaller, *Polyhedral realizations of developments* (in Russian) Vestnik Leningrad Univ. 15, pp 66–80 (1960)

[**BZ2**] Y. D. Burago and V. A. Zalgaller, *Isometric piecewise-linear embeddings of two-dimensional manifolds with a polyhedral metric into* $\boldsymbol{R}^3$, Algebra i Analiz **7**(3), pp 76–95 (1995). English translation: St. Petersburg Math. J. **7**(3), pp 369–385 (1996).

[**DS**] P. Doyle and R. E. Schwartz, *Collapsibility and Near Universality for Vertex Minimal Paper Tori*, arXiv:2510.12623 (2025)

[**L**] F. Lander, *The Two Most Symmetric Flat Tori as Eight-Vertex Paper Tori*, arXiv:2609.10703 (2026)

[**LT**] F. Lazarus, F. Tallerie, *A Universal Triangulation for Flat Tori*, Discrete and Computational Geometry **71** (2024) pp 278–307

[**S1**] R. E. Schwartz, *Vertex Minimal Paper Tori*, arXiv 2507.14998 (2025)

[**S2**] R. E. Schwartz, *The Most Efficient Origami Torus*, P.N.A.S. **123** (21) (2026)

[**S3**] R. E. Schwartz, *The Projective Heat Map*, Mathematical Surveys and Monographs **219**, American Mathematical Society, 2017.

[**Se**] H. Segerman, *Visualizing Mathematics with 3D Printing*, Johns Hopkins U. Press (2016)

[**T**] T. Tsuboi, *On origami embeddings of flat tori*, arXiv 2007.03434 (2020)

[**W**] Wolfram Research, Inc., *Mathematica*, Wolfram Research, Inc., Champaign, IL, `https://www.wolfram.com/mathematica`